INTERNATIONAL JOURNAL FOR NUMERICAL METHODS IN FLUIDS
Int. J. Numer. Meth. Fluids (2016)
Published online in Wiley Online Library (wileyonlinelibrary.com). DOI: 10.1002/fld.4247

Ensemble data assimilation applied to an adaptive mesh ocean model

Juan Du[1,*,†], Jiang Zhu[1], Fangxin Fang[2], C. C. Pain[2] and I. M. Navon[3]

[1]*International Center for Climate and Environment Science, Institute of Atmospheric Physics, Chinese Academy of Sciences, Beijing 100029, China*
[2]*Department of Earth Science and Engineering, Applied Modelling and Computation Group, Imperial College London, London SW7 2BP, UK*
[3]*Department of Scientific Computing, Florida State University, Tallahassee, FL 32306-4120, USA*

SUMMARY

In this study, a first attempt has been made to introduce mesh adaptivity into the ensemble Kalman fiter (EnKF) method. The EnKF data assimilation system was established for an unstructured adaptive mesh ocean model (Fluidity, Imperial College London). The mesh adaptivity involved using high resolution mesh at the regions of large flow gradients and around the observation points in order to reduce the representativeness errors of the observations. The use of adaptive meshes unavoidably introduces difficulties in the implementation of EnKF. The ensembles are defined at different meshes. To overcome the difficulties, a supermesh technique is employed for generating a reference mesh. The ensembles are then interpolated from their own mesh onto the reference mesh. The performance of the new EnKF data assimilation system has been tested in the Munk gyre flow test case. The discussion of this paper will focus on (a) the development of the EnKF data assimilation system within an adaptive mesh model and (b) the advantages of mesh adaptivity in the ocean data assimilation model. Copyright © 2016 John Wiley & Sons, Ltd.

Received 7 December 2015; Revised 23 March 2016; Accepted 21 April 2016

KEY WORDS: adaptive mesh; supermesh; EnKF; data assimilation; conservative interpolation; ocean modelling

1. INTRODUCTION

A grand challenge in ocean models is modelling the global circulation across the full range of relevant spatial and temporal scales [1]. For ocean prediction, this means resolving both basin scale and smaller scale features such as boundary currents, mixing, chemical interactions and transport, overflows and mesoscale eddies. These features often have spatial resolutions of 10 km or smaller and evolve over thousands of years. Such simulations are beyond the capability of traditional ocean models. Over the last decade, an important contribution to improving the resolution of ocean models has involved the introduction of unstructured meshes. Unstructured, dynamically adaptive mesh models can efficiently resolve global, basin, regional and small-scale flow structures. Newly developed adaptive unstructured mesh models offer significant advantages over the traditional models because they are the only techniques that can simultaneously resolve both small and large scale flows. The use of adaptive unstructured meshes will also reduce computational cost and increase accuracy.

One of the most important tasks for unstructured mesh ocean modelling [2] is to develop data assimilation methods along with reliable error norms. Data assimilation techniques in ocean modelling provide a quantitative, objective method to infer the state of the ocean system from

*Correspondence to: Juan Du, International Center for Climate and Environment Science, Institute of Atmospheric Physics, Chinese Academy of Sciences, Beijing 100029, China.
†E-mail: dujuan10@mail.iap.ac.cn

heterogeneous, irregularly distributed and temporally inconsistent observational data. Adaptive meshing methods in combination with data assimilation are capable of producing a best estimate model solution by refining a numerical simulation in the presence of the observational data over both space and time [3]. This provides a better description of the model (ocean) state over time than that provided by the raw observations, thus increasing our understanding of oceanic behaviour. The increased understanding has, in turn, led to the development of improved numerical models.

Variational data assimilation techniques are widely used in operational modelling. This includes the computationally economical 3D variational methods which exclude the flow dependent forecast errors [4] and the computationally demanding but very powerful 4D variational methods which require availability of an adjoint model [5]. An alternative method is ensemble Kalman filtering (EnKF) introduced in 1994 [6], which is useful because it is easy to implement (no adjoint models are required), along with its potential for efficient use on parallel computers with large-scale geophysical models [7, 8].

The EnKF is based on a Monte Carlo approach, using an ensemble of model representations to build up the necessary statistics [9, 10]. A background error covariance is computed using an ensemble of forecasts, with the current analysis ensemble serving as initial conditions. The EnKF then updates the analysis ensemble from observations. The EnKF is easy to implement and handles strong nonlinearities better than other known Kalman filter techniques for large-scale problems [11]. Several types of ensemble-based Kalman filter algorithms have been developed using either stochastic (perturbed observations) or deterministic (square root) filters. Some discussions of ensemble-based data assimilation methods are discussed in [4, 12–14]. A wealth of examples of practical applications could be found in [15–23].

In this work, the stochastic EnKF approach has been implemented for an adaptive mesh ocean model (Fluidity) that can simultaneously resolve both small-scale and large-scale ocean flows while smoothly varying mesh resolution and conforming to complex coastlines and bathymetry [2, 24–27]. What distinguishes the EnKF model developed here from other existing EnKF models is the inclusion of an adaptive mesh capability. This represents the main challenge in the implementation of the EnKF approach. For data assimilation in conjunction with adaptive mesh, the unstructured adaptive mesh ocean models have the advantage of using high resolution around the observation points in order to reduce the representativeness errors of observations. When adaptive meshes are employed, the mesh resolution requirements may be spatially and temporally different, as the meshes are adapted according to the flow features. This unavoidably introduces difficulties in the implementation of EnKF for an adaptive model. One of these challenges is that ensemble can be of different lengths at different time levels. To overcome these difficulties, a standard reference fixed mesh is adopted for EnKF. The ensembles are then interpolated from their own mesh onto the reference fixed mesh.

However, this also introduces an interpolation error into ensembles and the EnKF system. The interpolation error may destroy conservation of quantities important to the physical accuracy of the simulation such as density, volume fractions or tracer concentrations [28]. To reduce the interpolation error, a supermesh technique is employed, where globally conservative interpolation operators between general unstructured meshes are used to construct an intermediate supermesh [29].

The application of supermesh to mesh adaptivity was first introduced by Farrell *et al.* [29, 30], who also described a bounded variant of the Galerkin projection for piecewise linear fields. The projection algorithm described is not the optimally accurate Galerkin projection and is specific to piecewise linear fields. However, it is conservative and bounded.

The remainder of this paper is structured as follows: In Section 2, EnKF is briefly described. In Section 3, the adaptive mesh model (Fluidity) is introduced. The mesh adaptivity and implementation of the EnKF model are discussed in detail in Section 4. In Section 5, the aforementioned EnKF system is applied to and illustrated using a typical ocean case: Munk Gyre. Summary and conclusions are drawn in the final section.

DOI: 10.1002/fld

2. KALMAN FITER METHOD DATA ASSIMILATION

The EnKF algorithms used here are based on the work of Evensen [10] and the analysis scheme from Burgers *et al.* [9].

The ensemble members are defined as $\psi_i \in \Re^n (i = 1, \cdots, N)$, where N is the ensemble size and n is the dimension of the model state. The ensemble matrix A can be constructed by the model states of the ensemble as:

$$A = (\psi_1, \psi_2, \cdots, \psi_N) \in \Re^{n \times N} \tag{1}$$

The anomaly matrix is

$$A' = A - \overline{A} \tag{2}$$

where $\overline{A}$ is the ensemble mean vector.

The observation vector is $d \in \Re^m$. Suppose its uncertainty is ϵ_j $(\Sigma = (\epsilon_1, \cdots, \epsilon_N))$. We can have the perturbed observations of N random vectors:

$$d_j = d + \epsilon_j, \quad j = 1, \cdots, N \tag{3}$$

where d_j conform to a N(d,R) Gaussian distribution. R is the observation error covariance matrix. The ensemble of the innovation vectors is defined as the matrix

$$D' = D - HA \tag{4}$$

where $D = (d_1, \cdots, d_N)$ and H is the observation operator which interpolates the model state to the observation space.

The forward integration for the model states can be written as

$$\psi_{k+1}^f = g\left(\psi_k^a\right) + q_k \tag{5}$$

where k is the time step and q_k is a random model error sampled independently from a Gaussian distribution. The operator g is a nonlinear function representing the model integration.

The analysis update equation is given in matrix form:

$$A^a = A + P_e H^T \left(HP_e H^T + R\right)^{-1} (D - HA) \tag{6}$$

where P_e is the background error covariance matrix of the ensembles.

The Kalman gain is

$$K = P_e H^T \left(HP_e H^T + R\right)^{-1} \tag{7}$$

The analysis update equation can be also written using only anomalies as

$$A^a = A + A' A'^T H^T \left(HA' A'^T H^T + \Sigma\Sigma^T\right)^{-1} D' \tag{8}$$

where A' is the anomaly matrix of the ensembles. Σ is the matrix of observation perturbations. D' is the innovation matrix.

For the implementation of EnKF with adaptive mesh, the essential problem is that the ensembles are defined on different meshes, which means that the dimensional size of the ensemble members are different and the ensemble matrix A can't be derived directly. Let the ensemble members be $\phi_i \in \Re^{n_i} (i = 1, \cdots, N)$, where N is the ensemble size and n_i is the dimension of the i_{th} ensemble member. By interpolating the ensembles ϕ_i to a fixed reference mesh, a set of ensemble members with the same dimension could be derived. Then the standard EnKF scheme could be applied to the ensembles as mentioned earlier. More details of the adaptive mesh EnKF scheme will be presented in Section 4.

3. AN UNSTRUCTURED MESH FLUID MODEL

In this work, the EnKF method was implemented for an unstructured adaptive mesh fluid model developed by Imperial College London, Fluidity) which is introduced later.

DOI: 10.1002/fld

3.1. Introduction to fluidity

Fluidity is a 3D non-hydrostatic fluid model which uses control volume finite element discretisation methods on meshes which may be unstructured in all three dimensions and which may also adapt to optimally resolve multiscale dynamics [24, 31].

There are significant potential advantages of an unstructured mesh fluid model [2]. For example, there are issues relating to boundary conditions when bathymetry and coastlines are represented by a 'staircase' regular structured mesh. The result can be an inadvertent application of no-slip boundary conditions and consequent problems with the transport of dense fluids along slopes. This process must be parameterised for staircase topography, for example, using enhanced diffusion in the cells adjacent to the ocean floor. Having the mesh aligned with the bathymetry avoids many of these problems [32] and allows the fluid to slide over bathymetry, as described by a frictional model for example. Unstructured meshes also enable the use of greater mesh resolution in the direction normal to the coastline than tangential to it where typically boundary layers develop (e.g. western and frictional). Resolving developing flow features (e.g. fronts, eddies and overflows) whose positions are not necessarily known a priori requires the use of adaptive mesh resolution. Thus, ideally mesh adaptivity techniques would be employed which can dynamically change model resolution to optimally resolve such flows.

Adaptive meshes in 3D space and time make it possible that regions of steep topography, high dynamical activity or specific interest can be modelled at a high horizontal and vertical resolution. The mixed finite element pair is adopted which is a first order discontinuous finite element for the velocity variable and a second order continuous finite element for the pressure, temperature and other state variables [33, 34]. Nonlinear advection methods on unstructured meshes are also exploited so that both accuracy and robustness may be combined.

3.2. Adaptive mesh techniques

A dynamically adapting anisotropic mesh in 3D is used here. Mesh adaptivity or optimisation relies on the derivation of appropriate error measures, which dictate how the mesh is to be modified [1, 24]. A metric tensor is used to calculate the required edge lengths and orientation of the mesh elements to control solution errors. It is constructed so that an ideal edge length is unity when measured in metric space. Because the metric is dependent on both location and direction, it is able to reflect locally anisotropic information within the solution. Thus, inhomogeneous and anisotropic meshes result from this approach. By defining an objective functional which is based on the element quality in this metric space, an optimisation technique is used to improve the overall quality of the mesh. Local operations based on a series of mesh connectivity and node position searches are performed on a 3D tetrahedral mesh and include: edge collapsing/splitting, face to edge and edge to face swapping, edge to edge swapping and local node movement or mesh smoothing in a fashion similar to [35] and [36]. Constraints are imposed on these operations so as to preserve the integrity of nonplanar geometrical boundaries [24].

To reduce the interpolation error, high-order interpolation approaches are employed [37]. For each node in the reference mesh, the element of the adapted mesh in which the node lies is identified. Then, a local higher-order polynomial (e.g. quadratic or cubic) is fitted with a least squares approach on a patch of nodes around this element. This polynomial is then evaluated at the location of the node in the reference mesh to determine the interpolated value. This scheme is more accurate than linear interpolation with a higher computational cost as a dense matrix must be inverted for each element in the original mesh to compute the interpolated solution.

4. IMPLEMENTATION OF ENSEMBLE KALMAN FILTER IN FLUIDITY AND SUPERMESH TECHNIQUES

4.1. Issue of implementation of ensemble Kalman filter in an adaptive mesh model

When adaptive meshes are employed, the mesh resolution requirements vary spatially and temporally, as the meshes are adapted according to the flow features through the whole simulation. The

DOI: 10.1002/fld

dimensional size of the variable vectors is different at each time level because the number of nodes varies during the simulation. Ensembles can therefore be of different length at different time levels. This unavoidably brings difficulties in the implementation of EnKF for an adaptive mesh model. To overcome these difficulties, a standard reference fixed mesh is adopted for the EnKF model. The solutions from the original model are interpolated from their own mesh onto the same reference fixed mesh at each time level, and then stored in the ensembles. This allows the same length of ensembles to be obtained at each time level. The resolution of the reference mesh and the interpolation errors between the two meshes (the adaptive mesh and the fixed reference mesh) may affect the accuracy of EnKF, and thus, the reference mesh must be chosen carefully so that it is at least as fine as the finest adapted mesh at a given location. To reduce the interpolation error, high-order interpolation approaches are employed. In this work, the reference mesh is obtained by the supermesh technique described thereafter. The adaptive mesh EnKF data assimilation scheme was shown in Figure 1.

4.2. Supermesh technique

The use of adaptive meshes introduces the different length of ensembles. The ensemble variables are defined on different meshes. To overcome the issue, a standard reference fixed mesh is adopted for EnKF. The ensembles are then interpolated from their own meshes onto the reference fixed mesh. However, the error caused by interpolating from the one mesh onto the reference fixed mesh could destroy conservation of quantities important to the physical accuracy of the simulation such as density, volume fractions or tracer concentrations. To avoid such problem, we employed here the conservative interpolation operators between general unstructured meshes via the construction of an intermediate supermesh.

The definition of a supermesh (Figure 2) has the following characteristics [30]. First, any node in a parent mesh must be present in the supermesh. Secondy, for every element in the supermesh, the intersection of that element with any element of a parent mesh must either be a set of measure zero or the whole element. Note that a supermesh is not unique. To construct a supermesh satisfying the aforementioned definition from two given input meshes, it is proven that the construction process may be converted to that of a constrained meshing problem. To solve a constrained triangulation

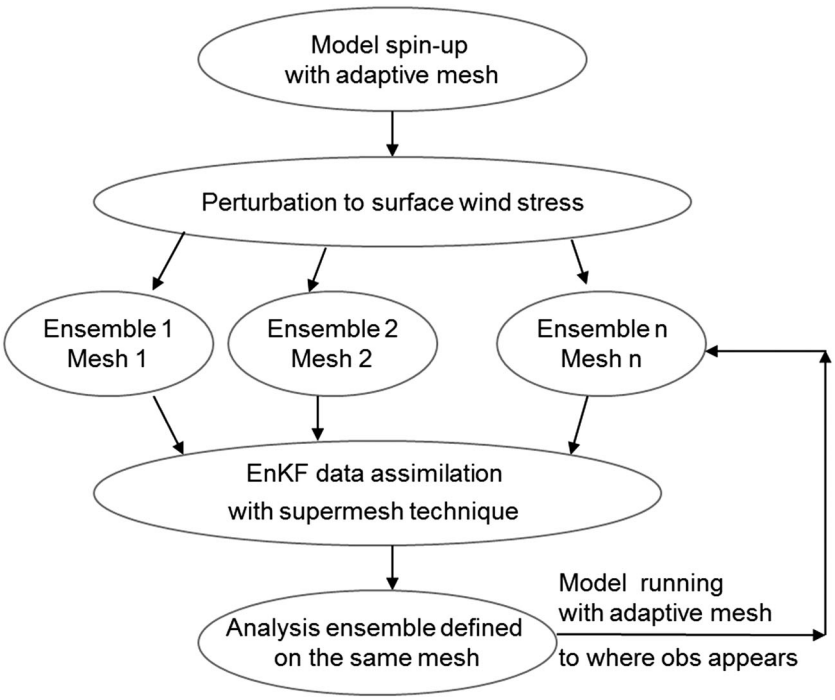

Figure 1. The adaptive mesh ensemble Kalman filter (EnKF) data assimilation scheme.

DOI: 10.1002/fld

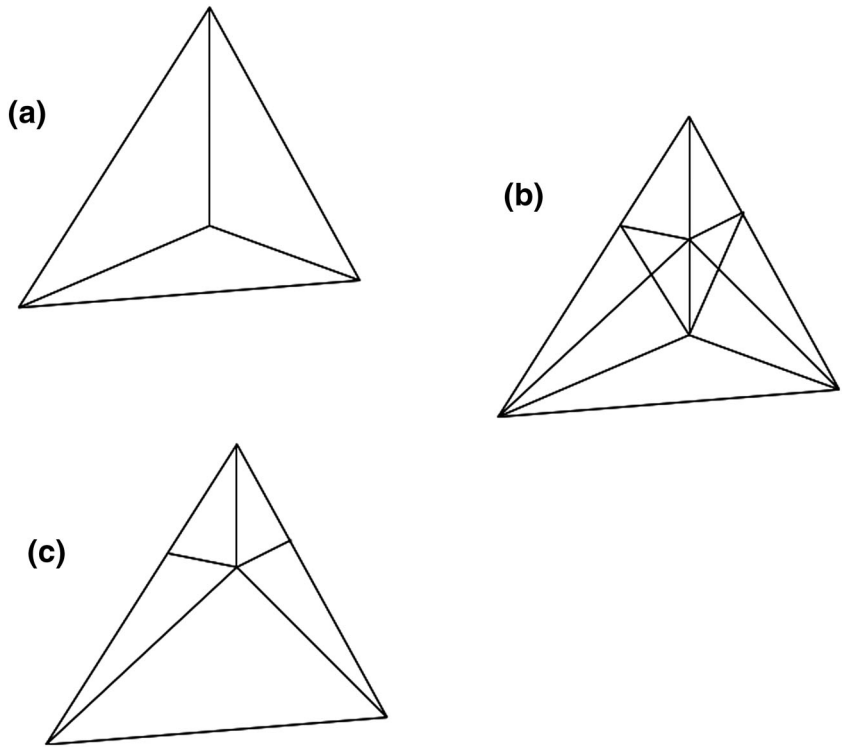

Figure 2. Supermesh construction, where (a) and (c) are two different meshes, and (b) is the supermesh constructed based on mesh (a) and mesh (b).

problem, some widely available, robust algorithms for the problems of computational geometry inherent in the conservative interpolation algorithms could be used.

The method of mesh to mesh interpolation [37] begins with a set of two meshes, one that represents an old mesh and the other that represents the new adapted one. It is expected that the new mesh will contain regions with different resolution than that of the previous one. Furthermore, in almost all cases, if the two meshes were to be superimposed onto each other, they would not overlap in a consistent manner so that volumes and surfaces are not resolved by both meshes. This is illustrated in Figure 2, which shows a cross section of the new mesh overlaid on top of the previous one. The adapted mesh is clearly shown to be represented in more detail, and there are several instances where previous mesh elements are only partially occupied by the new mesh. During the eigenvalue solving procedure, when a mesh is adapted the flux on the old mesh is required to be mapped onto the new mesh in a consistent and conservative way. The mesh interpolation approach consists in using a Galerkin projection of the geometries over a supermesh, which is generated by the overlapping of the old and new meshes. An example of a supermesh is presented in Figure 2, and this shows how new elements are formed from the intersections of all lines (and surfaces for 3D) of both meshes. Although these elements are not of regular type associated with finite elements, they do have the important property that they contain only a single volume. This supermesh therefore enables one to map flux information between the two meshes because each of its elements (containing a single volume) can be fully mapped onto a single element associated with either the old or new mesh. It is therefore a simple task of correctly interpolating the old mesh information onto the new mesh.

4.3. Test case: 3D wind-driven ocean circulation case

The domain for the wind-driven ocean circulation model is 1500 km $\times$ 1500km in the horizontal direction and 1 km in the vertical direction. Only ocean surface wind forcing boundary condition is applied. The wind stress is given as the cosine function of the horizontal x coordinate. The Coriolis terms are taken into account with the beta-plane approximation. State variables to construct

DOI: 10.1002/fld

the ensemble matrix are velocity (u,v and w) and sea surface height (h). The surface 2D mesh is composed with unstructured triangular elements, which are extruded to the domain bottom with only one layer in the vertical direction. A high resolution model with an uniform element length of 5 km in the horizontal direction (experiment 1 in Table I) is setup as a reference result, from which the sea surface height solutions at some given locations are derived as the observation information for the EnKF data assimilation experiments. The designed observations were assimilated into the same ocean model with a low resolution fixed mesh (20 km) and biassed wind forcing ocean model (experiment 2 in Table I) after spinning up for two years. Another data assimilation experiment (Experiment 3 in Table I) is similar to experiment 2 except that the mesh is adaptive w.r.t. the velocity variable with the element side length limited between 5km and 20km. Considering the mesh refinement around the observation locations, the mesh is adaptive w.r.t. both the velocity variable and the observation locations in experiment 4. Different observation errors are applied to the fixed and adaptive mesh experiments. The detailed setup of the data assimilation experiments is shown in Table I.

The observation locations are designed as the intersections of several tracks inside the domain surface (Figure 3). There are 41 observation locations throughout the whole domain.

4.3.1. Ensemble Kalman fiter method experiments with unstructured fixed mesh. The construction of the unstructured mesh EnKF data assimilation system starts with a low resolution (20 km) fixed mesh ocean model. The setup of the low-resolution model is the same with the high-resolution model except the horizontal mesh resolution and the surface wind forcing. The 20 km low resolution model (experiment 2) is forced by a biassed surface wind, which is necessary to generate a relatively biassed model solution compared with the 5 km high-resolution model (experiment 1). The observation information derived from the high-resolution model is then assimilated into the biassed low-resolution model using the EnKF data assimilation method. The assimilation took place

Table I. Experiments setup.

Index	Mesh	Resolution	Wind stress	Observations	DA period
Experiment 1	Fixed	5 km	True	N/A	N/A
Experiment 2	Fixed	20 km	Biassed	41 Locations	730–1100 days
Experiment 3	Adaptive w.r.t. velocity	5km–20 km	Biassed	41 Locations	730–1100 days
Experiment 4	Adaptive w.r.t. velocity and obs. Locations	5km–20 km	Biassed	41 Locations	730–1100 days

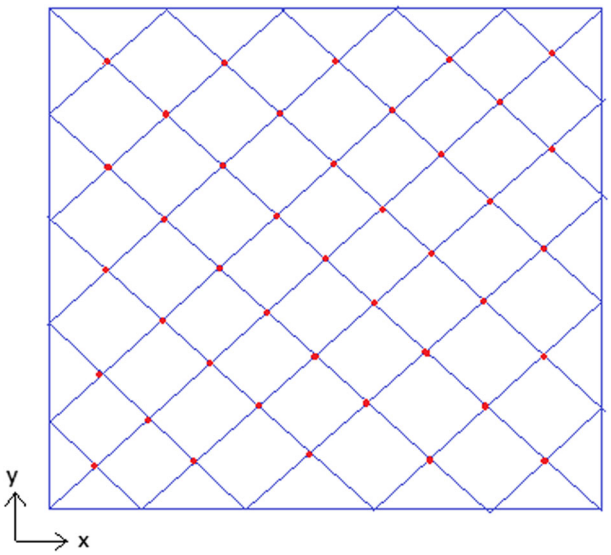

Figure 3. Designed observation locations.

DOI: 10.1002/fld

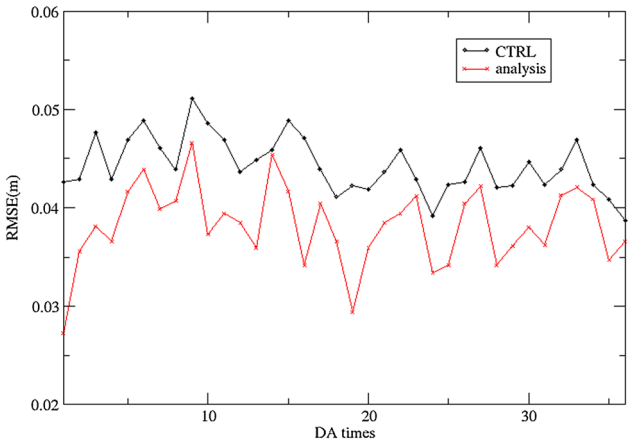

Figure 4. Error in free surface height (unit: m), before (marked as 'CTRL') and after (marked as 'analysis') ensemble Kalman fiter method data assimilation. RMSE, root mean square error.

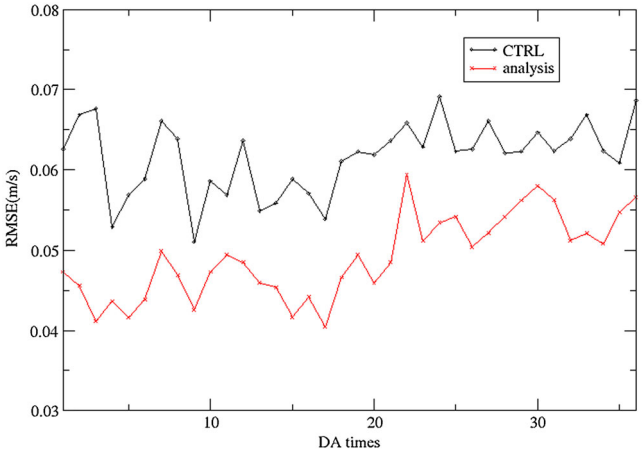

Figure 5. Error in the x-direction component of velocity (unit: m/s), before (marked as 'CTRL') and after (marked as 'analysis') ensemble Kalman filter (EnKF) data assimilation.

every 10 days with the mesh fixed at all the time levels. Figure 4 shows that the root mean square error (RMSE) of the free surface height before (marked as 'CTRL') and after (marked as 'analysis') the EnKF data assimilation process. It can be seen that the EnKF data assimilation system has a good impact on the model integration compared with the observations we generated using a high-resolution twin experiment. Similar results are shown in Figure 5 for the velocity component in the x-direction. Based on this, we can extend the construction of the unstructured mesh EnKF data assimilation system to adaptive mesh ocean model.

The RMSE is defined as follows:

$$\epsilon_r = \sqrt{\frac{1}{N}\sum_{i=1}^{N}\left(x_i - x_i^o\right)^2} \tag{9}$$

where N denotes the number of observations, x_i represents the model state and x_i^o represents the i-th observation.

4.3.2. Ensemble Kalman fiter method experiments with unstructured adaptive mesh. When we run the ocean model using adaptive meshes, we got the ensembles defined on different meshes. The EnKF data assimilation process with adaptive meshes involves the following key points.

DOI: 10.1002/fld

First of all, the observation mesh (structured mesh, triangle format) was generated according to the designed observation locations, and the unstructured surface mesh of the computation domain was interpolated to the observation mesh. This step is essential to calculate the observation innovation. Secondly, adaptive mesh was adopted for every initial ensemble and then interpolated to one 'optimal' mesh when encountering an observation, where the supermesh technique is adopted. Furthermore, the mesh around the observation locations could be refined adaptively to reduce the representative error (Figure 6) and to improve the assimilation effect.

Figure 7 shows details of adaptive meshes of one ensemble member at different time steps. The mesh is adapted every 10 days. The allowed maximum mesh element side length is 20 km, and the allowed minimum is 5 km, which limited the adaptive mesh resolution between the low resolution (20 km) of the fixed mesh data assimilation experiment as descried in the previous section and the high resolution (5 km) of the reference model integration.

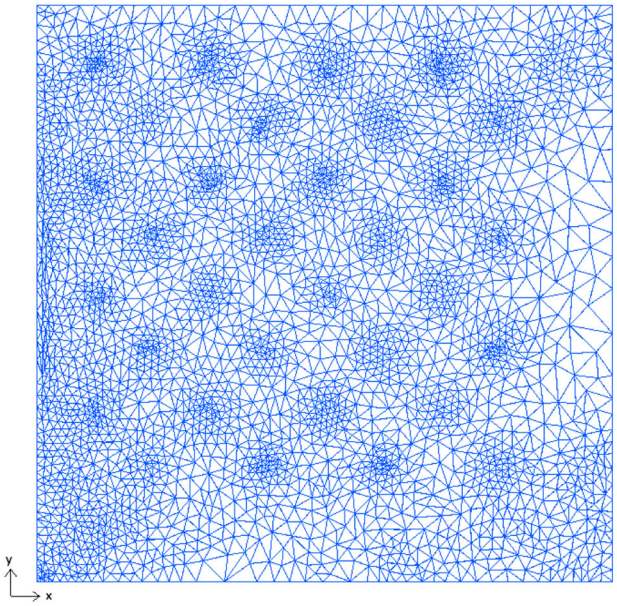

Figure 6. Surface mesh adapted according to the observation locations.

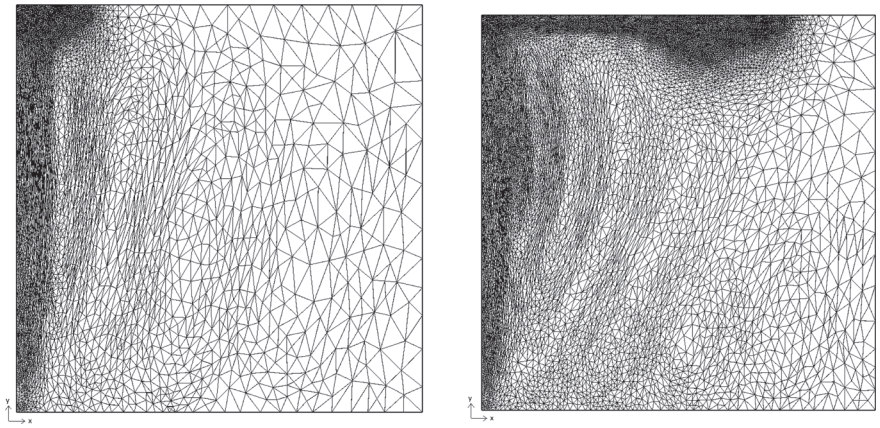

(a) Adapted mesh at 300 day simulation (b) Adapted mesh at 600 day simulation

Figure 7. Adapted mesh according to velocity. (a) Adapted mesh at 300-day simulation and (b) Adapted mesh at 600-day simulation.

DOI: 10.1002/fld

Figures 8 and 9 show the RMSE of the assimilated variables free surface height and the x-direction component of velocity, respectively, before and after the EnKF data assimilation process with the adaptive mesh. We can see that the model results with adaptive mesh (experiment 3) are already better than that without adaptive mesh (experiment 2, Figure 4) compared with the observations derived from the high-resolution ocean model (experiment 1) before the data assimilation process. In the data assimilation process, the observation information was assimilated into the biassed low resolution model every 10 days. The data assimilation experiments last for 1 year after the initial ensembles were generated. From Figure 8, we can see that the RMSE were effectively reduced every time the observation information was present during the data assimilation process. This proves that the adaptive mesh EnKF data assimilation system has a positive impact on the numerical model with the present of observations, which is the foundation of applying the adaptive mesh data assimilation system to realistic ocean model with real observations, including both the conventional and satellite observations. Similar conclusion could be derived from Figure 9 and also from the other assimilated state variables.

In experiment 4, the unstructured mesh was adapted with respect to both the velocity variable and the observation locations (Figure 6). The mesh resolution around the observation locations was relatively high in order to reduce the representativeness errors of observations. The RMSE before and after EnKF data assimilation for the free surface height and the x-direction component

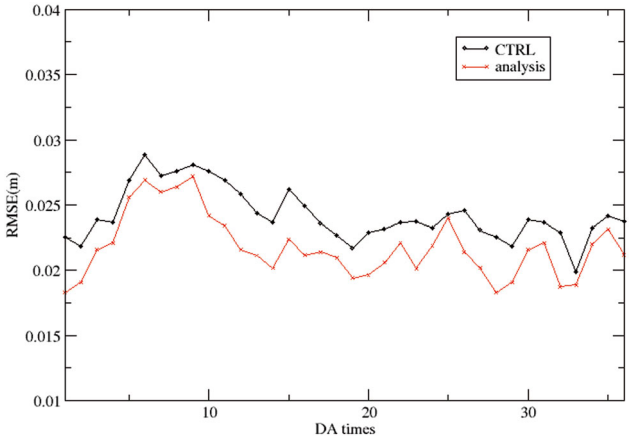

Figure 8. Error in free surface height (unit: m), before (marked as 'CTRL') and after (marked as 'analysis') ensemble Kalman fiter method data assimilation. RMSE, root mean square error.

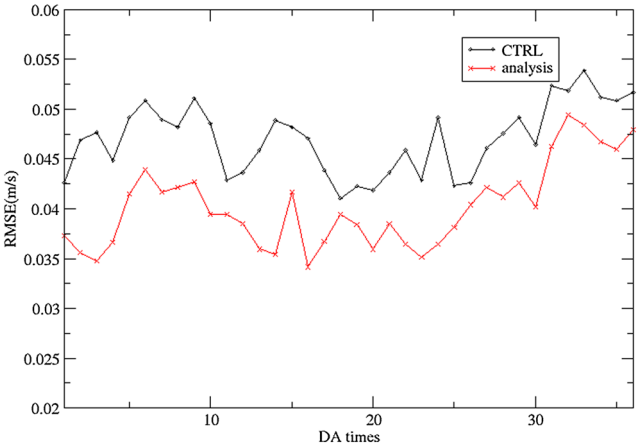

Figure 9. Error in the x-direction component of velocity (unit: m/s), before (marked as 'CTRL') and after (marked as 'analysis') ensemble Kalmandata assimilation.

DOI: 10.1002/fld

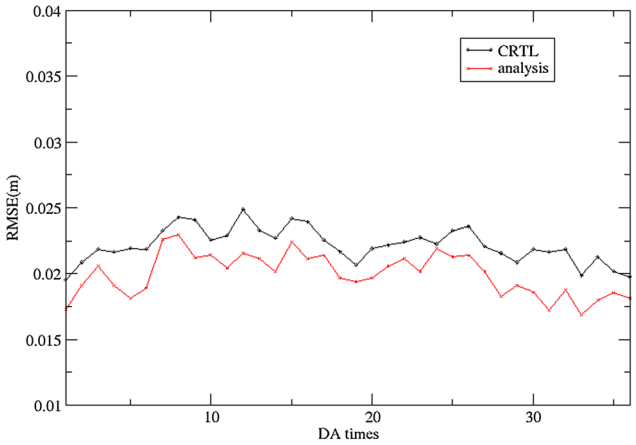

Figure 10. Error in free surface height (unit: m), , before (marked as 'CTRL') and after (marked as 'analysis') ensemble Kalman filter data assimilation. RMSE, root mean square error.

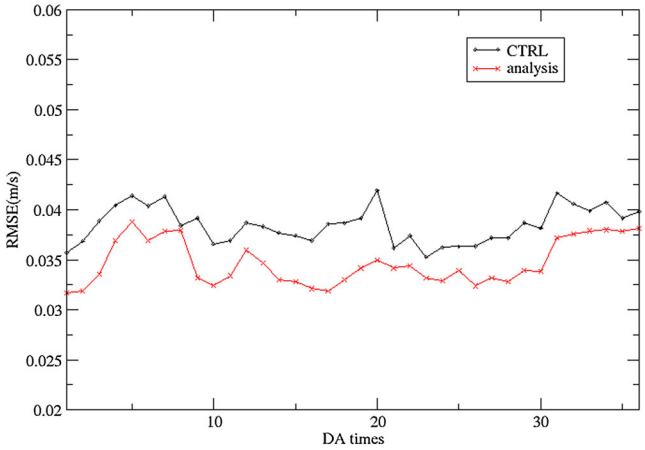

Figure 11. Error in the x-direction component of velocity (unit: m/s), before (marked as 'CTRL') and after (marked as 'analysis') ensemble Kalman filter data assimilation. RMSE, root mean square error.

of velocity are shown in Figures 10 and 11, respectively. It could be seen that before the EnKF data assimilation, the error between the numerical model and the observations was further reduced compared with the result shown in Figures 8 and 9, respectively, with the improvement of increasing the mesh resolution around the observation locations. After the EnKF data assimilation process, the error was further reduced, which proves the effectiveness of the adaptive mesh data assimilation system. Similar results were obtained for the other assimilated state variables.

5. CONCLUSIONS

Data assimilation with unstructured adaptive mesh ocean model is attractive due to two reasons. First, unstructured adaptive mesh ocean models have the advantages of using high-resolution mesh at the regions of large flow gradients or nonsmooth coastlines to better approximate the continuous flow. Secondly, for data assimilation, the unstructured adaptive mesh ocean models have an additional advantage of using high resolution around the observation points in order to reduce the representativeness errors of observations. In this study, we illustrate the aforementioned ideas using Fluidity/ICOM model in identical twin experiments, in which model simulated altimetry data are assimilated by ensemble Kalman filter. Because one ensemble member could be defined at a different mesh from another ensemble member, it is not straightforward to apply the ensemble Kalman

DOI: 10.1002/fld

filter to adaptive mesh models. A supermesh method is applied to overcome the technical problem. It is proven that the adaptive mesh EnKF data assimilation system has a positive impact on the numerical model, which is the foundation of applying the adaptive mesh data assimilation system to realistic ocean model with real observations, including both the conventional and satellite observations. The mesh adaptivity (increased mesh resolution) around the observation locations improved the model results further by assimilating the observations, which could be applied to the ensemble data assimilation of the realistic ocean modelling considering the importance of reducing the representative error around the observation locations.

ACKNOWLEDGEMENTS

Dr. Juan Du acknowledges the support of the National Natural Science Foundation of China (Grant No. 41406037).

REFERENCES

1. Ford R, Pain CC, Piggott MD, Goddard AJH, de Oliveira CRE, Umbleby AP. A nonhydrostatic finite-element model for three-dimensional stratified oceanic flows. Part I: model formulation. *Monthly Weather Review* 2004; **132**(12):2816–2831.
2. Pain CC, Piggott MD, Goddard AJH, Fang F, Gorman GJ, Marshall DP, Eaton MD, Power PW, de Oliveira CRE. Three-dimensional unstructured mesh ocean modelling. *Ocean Modelling* 2005; **10**(12):5–33.
3. Fang F, Pain CC, Navon IM, Piggott MD, Gorman GJ, Farrell PE, Allison PA, Goddard AJH. A POD reduced-order 4D-Var adaptive mesh ocean modelling approach. *International Journal for Numerical Methods in Fluids* 2009; **60**:709–732.
4. Blum J, Le Dimet FX, Navon IM. Data assimilation for geophysical fluids. In *Chapter in Computational Methods for the Atmosphere and the Oceans*, Vol. 14: Special Volume of Handbook of Numerical Analysis, Temam R, Tribbia J (eds). Elsevier Science Ltd: New York, 2009; 784 pages. ISBN-13: 978-0-444-51893-4 (Philippe G. Ciarlet, Editor).
5. Du J, Navon IM, Zhu J, Fang F, Alekseev AK. Reduced order modeling based on POD of a parabolised Navier–Stokes equations model II: trust region POD 4D VAR data assimilation. *Computers and Mathematics with Applications* 2013; **65**:380–394.
6. Evensen G. Sequential data assimilation with a nonlinear quasi-geostrophic model using Monte Carlo methods to forecast error statistics. *Journal of Geophysical Research* 1994; **99**:10,143–10,162.
7. Evensen G, Jan van Leeuwen P. Assimilation of Geosat Altimeter data for the Agulhas current using the ensemble Kalman filter with a Quasi-Geostrophic model. *Monthly Weather Review* 1996; **124**:85–96.
8. Nerger L, Hiller W, Schroter J. PDAF - the parallel data assimilation framework: experiences with Kalman filtering. In *Use of High Performance Computing in Meteorology- Proceedings of the 11. ECMWF Workshop*, Zwieflhofer W, Mozdzynski G (eds). World Scientific: Reading, UK, 2005; 63–83.
9. Burgers G, Evensen G, Jan van Leeuwen P. On the analysis scheme in the ensemble Kalman filter. *Monthly Weather Review* 1998; **126**:1719–1724.
10. Evensen G. The ensemble Kalman filter: theoretical formulation and practical implementation. *Ocean Dynamics* 2003; **53**:343–367.
11. Sakov P, Oliver DS, Bertino L. An iterative EnKF for strongly nonlinear systems. *Monthly Weather Review* 2011; **140**:1988–2004.
12. Kalnay E. *Atmospheric Modeling, Data Assimilation and Predictability*. Cambridge University Press: Cambridge, UK, 2003. 341 pp.
13. Ott E, Hunt BR, Szunyogh I, Zimin AV, Kostelich EJ, Corazza M, Kalnay E, Patil DJ, Yorke JA. A local ensemble Kalman filter for atmospheric data assimilation. *Tellus* 2004; **56A**:415–428.
14. Sakov P, Evensen G, Bertino L. Asynchronous data assimilation with the EnKF. *Tellus* 2010; **62A**:24–29.
15. Bleck R, Boudra D. Initial testing of a numerical ocean circulation model using a hybrid (quasi-isopycnic) vertical coordinate. *Journal of Physical Oceanography* 1981; **11**:755–770.
16. Counillon F, Bertino L. High-resolution ensemble forecasting for the Gulf of Mexico eddies and fronts. *Ocean Dynamics* 2009; **59**:83–95.
17. Cummings J, Bertino L, Brasseur P, Fukumori I, Kamachi M, Martin MJ, Mogensen K, Oke P, Testut CE, Verron J, Weaver A. Ocean data assimilation systems for GODAE. *GODAE Special Issue Feature* 2009; **22**:96–109.
18. Oke PR, Allen JS, Miller RN, Egbert GD, Kosro PM. Assimilation of surface velocity data into a primitive equation coastal ocean model. *Journal of Geophysical Research* 2002; **107**:3122.
19. Oke PR, Schiller A, Griffin DA, Brassington GB. Ensemble data assimilation for an eddy-resolving ocean model of the Australia Region. *Quarterly Journal of the Royal Meteorological Society* 2005; **131**:3301–3311.
20. Vialard J, Vitart F, Balmaseda MA, Stockdale TN, Anderson DLT. An ensemble generation method for seasonal forecasting with an ocean-atmosphere coupled model. *Monthly Weather Review* 2005; **133**(2):441–453.
21. Wu CR, Shaw PT, Chao SY. Assimilation altimetric data into a South China Sea model. *Journal of Geophysical Research* 1999; **104**:29987–30005.

DOI: 10.1002/fld

22. Xie JP, Zhu J. Ensemble optimal interpolation schemes for assimilating Argo profiles into a hybrid coordinate ocean model. *Ocean Modelling* 2010; **33**:283–298.
23. Xie JP, Counillon F, Zhu J, Bertino L. An eddy resolving tidal-driven model of the South China Sea assimilating along-track SLA data using the EnOI. *Ocean Science* 2011; **7**:609–627.
24. Pain CC, Umpleby A, de Oliveira C, Goddard A. Tetrahedral mesh optimisation and adaptivity for steady-state and transient finite element calculations. *Computer Methods in Applied Mechanics and Engineering* 2001; **190**: 3771–3796.
25. Danilov S, Kivman G, Schroter J. A finite element ocean model: principles and evaluation. *Ocean Modelling* 2004; **6**:125–150.
26. Fix GJ. Finite element models for ocean circulation problems. *SIAM Journal on Applied Mathematics* 1975; **29**: 371–387.
27. Maddison JR, Marshall DP, Pain CC, Piggott MD. Accurate representation of geostrophic and hydrostatic balance in unstructured mesh finite element ocean modelling. *Ocean Modelling* 2011; **39**:248–261.
28. Simpson RB. Anisotropic mesh transformations and optimal error control. *Applied Numerical Mathematics* 1994; **14**(1–3):183–198.
29. Farrell PE. Galerkin projection of discrete fields via supermesh construction. *PhD Thesis*, Imperial College London, 2009.
30. Farrell PE, Maddison J. Conservative interpolation between volume meshes by local Galerkin projection. *Computer Methods in Applied Mechanics and Engineering* 2011; **200**(14):89–100.
31. Haidvogel DB, Beckmann A. *Numerical Ocean Circulation Modeling*. Imperial College Press: London, UK, 1999.
32. Adcroft A, Marshall D. How slippery are piecewise-constant coastlines in numerical ocean models? *Tellus* 1998; **A50**:95–108.
33. Du J, Fang F, Pain CC, Navon IM, Zhu J, Ham DA. POD reduced-order unstructured mesh modelling applied to 2D and 3D fluid flow. *Computers and Mathematics with Applications* 2013; **65**:362–379.
34. Fang F, Pain CC, Navon IM, Piggott MD, Gorman GJ, Allison PA, Goddard AJH. Reduced-order modelling of an adaptive mesh ocean model. *International Journal for Numerical Methods in Fluids* 2009; **59**:827–851.
35. Freitag LA, Gooch CO. Tetrahedral mesh improvement using swapping and smoothing. *International Journal for Numerical Methods in Engineering* 1997; **40**:3979–3999.
36. Buscaglia GC, Dari EA. Anisotropic mesh optimisation and its application in adaptivity. *International Journal for Numerical Methods in Engineering* 1997; **40**:4119–4136.
37. Baker CMJ, Buchan AG, Pain CC, Farrell PE, Eaton MD, Warner P. Multimesh anisotropic adaptivity for the Boltzmann transport equation. *Annals of Nuclear Energy* 2013; **53**:411–426.

DOI: 10.1002/fld